Spin Lattice Relaxation in Solution and Summary of Relaxation Mechanisms

Gareth R. Eaton and Sandra S. Eaton
Department of Chemistry and Biochemistry
University of Denver

Retie, Belgium
Dec. 1-7, 2002

What can you learn from measuring T_1 and T_2 in solution?

- Dynamics of molecular tumbling
- Oximetry
- Mechanisms of relaxation
  - Spin rotation
  - Modulation of g and/or A anisotropy
  - Modulation of zero-field splitting

Background Information

Early work by CW saturation on Fremy's salt gave $T_1 = T_2 =$ 0.5 μs.

Early work by saturation recovery, mostly of semiquinones by Rengen and later studies by Hyde and co-workers on nitroxyl radicals also yielded values in the μs range.

The rest of the early work on relaxation came largely from low temperature solid state physics.

There developed a dichotomy – solid state effects vs. effects relevant to the fast motional limit.

We have a research program that seeks to find the most important contributions to relaxation in the intermediate region where many EPR studies are performed.

Experimental Methods

In principle, any of the methods discussed for solids could be applied in solution. However, for many samples T_2 in fluid solution is so short that it is difficult to perform spin echo experiments. As a result, measurements of relaxation times in fluid solution typically are done by the following methods.

Saturation recovery curves can be measured even when T_2 is too short for spin echo formation.

Power saturation curves can be measured on a CW spectrometer. Disadvantages are that a) the saturation behavior depends on the product T_1T_2 and b) the saturation may be strongly impacted by spectral diffusion.

If the CW lineshape is dominated by incomplete motional averaging, T_2 can be determined from the linewidth after simulation including any unresolved hyperfine splitting.

Nitroxyl Tumbling Correlation Time

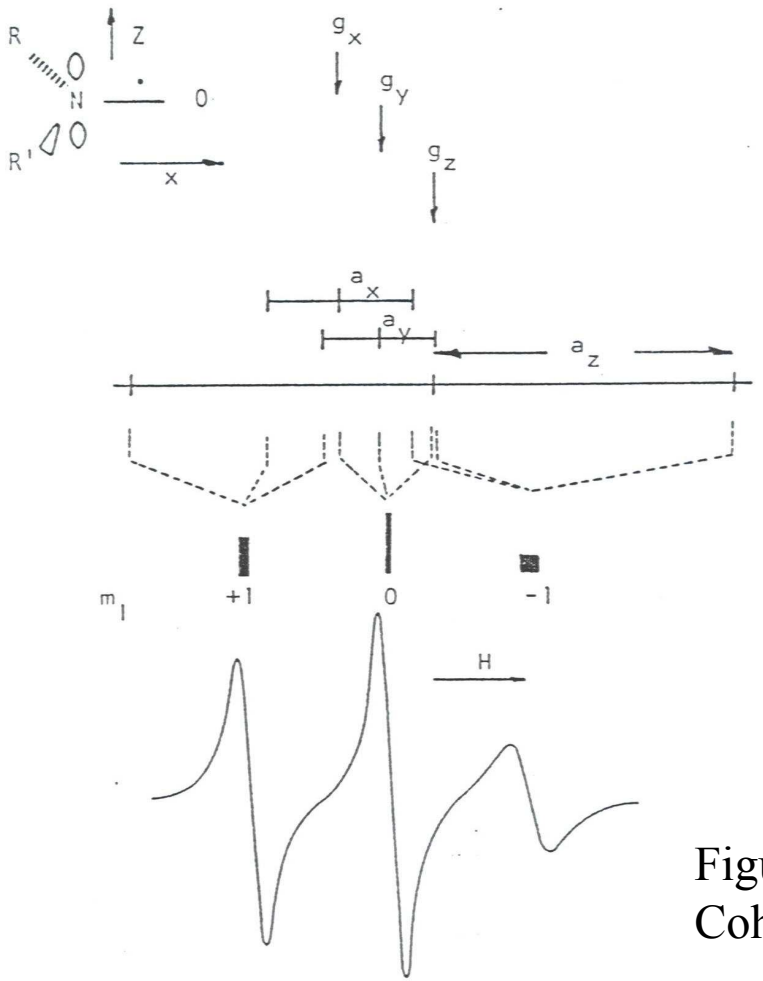

The nitroxyl g and A values along the x, y, and z axes are anisotropic. At X-band, the differences between the resonances along the three axes decrease in the order $m_I = -1 > +1 > 0$.

As the molecule tumbles, the smaller splitting for $m_I = 0$ is averaged more effectively than the larger splittings, which causes differences in the linewidths of the three hyperfine lines.

Figure adapted A. D. Keith, M. Sharnoff, G. E Cohn, *Biochim. Biophys. Acta* **300**, 379 (1973).

Nitroxyl Lineshapes

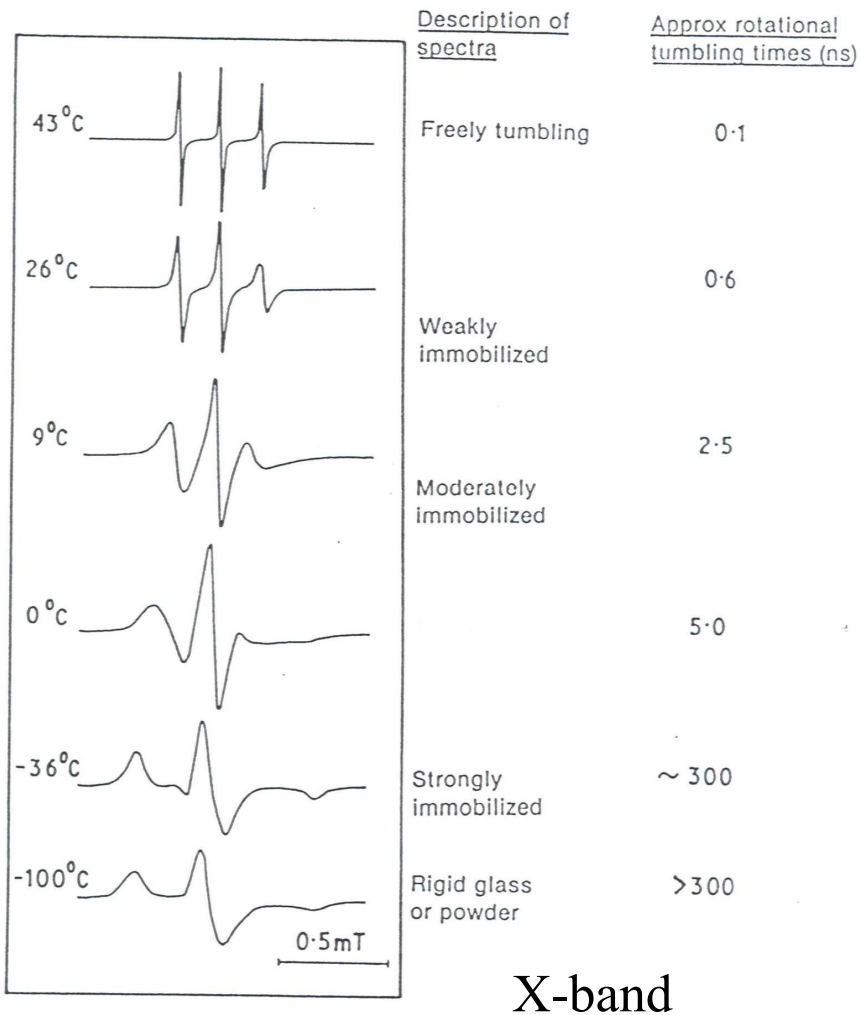

X-band

As the tumbling correlation time decreases, the extent of averaging of anisotropic features increases and the spectrum approaches the 3-line signal that is characteristic of rapid tumbling.

In the motional narrowing region, the dependence of the width of an individual hyperfine line on the nuclear spin state (m_I) can be expressed as

$$\Delta B(m_I) = A + B\,m_I + C\,m_I^{\,2}$$

The example on the following page assumes isotropic tumbling.

I. D. Campbell and R. A. Dwek, *Biological Spectroscopy,* Benjamin-Cummings, 1984, p. 192

Calculation of Tumbling Correlation Time

The parameters B and C are related to peak-to-peak amplitudes, $I(m_I)$ by:

$$B = \frac{1}{2}\left[\sqrt{\frac{I(0)}{I(+1)}} - \sqrt{\frac{I(0)}{I(-1)}}\right] \qquad C = \frac{1}{2}\left[\sqrt{\frac{I(0)}{I(+1)}} + \sqrt{\frac{I(0)}{I(-1)}} - 2\right]$$

The high-field line has $m_I = -1$.
Tumbling correlation times are calculated from B and C using

$$\tau = B\left[\left(\frac{2\hbar}{\sqrt{3}g_o\beta}\right)\left(\frac{4B_o}{15}\right)(b\Delta\gamma)\left(\frac{1}{\Delta B_o}\right)\right]^{-1} \quad \text{and} \quad \tau = C\left[\left(\frac{2\hbar}{\sqrt{3}g_o\beta}\right)\left(\frac{b^2}{8}\right)\left(\frac{1}{\Delta B_o}\right)\right]^{-1}$$

Where $g_o = \frac{1}{3}(g_x + g_y + g_z)$ $\qquad B_o = \frac{\hbar\omega}{g_o\beta}$

$$\Delta\gamma = \frac{\beta(g_z - 0.5(g_x + g_y))}{\hbar} \qquad b = \frac{2}{3}(A_z - 0.5(A_x + A_y))$$

ΔB_o is the peak-to-peak width of the center line
Hyperfine values (A) are in radians/s
The calculation assumes isotropic tumbling

D. Kivelson, *J. Chem. Phys*. **33**, 1094 (1960).
R. Wilson and D. Kivelson, *J. Chem. Phys*. **44**, 154 (1966)
N. D. Chasteen, *J. Phys. Chem*. **76**, 3951 (1972).

Sample Calculation

4-OH-TEMPO (tempol) in 9:1 glycerol:water

$g_x = 2.0103$, $g_y = 2.0067$, $g_z = 2.0032$

$A_x = 2\pi\ 18\text{x}10^6$, $A_y = 2\pi\ 22.5\text{x}10^6$, $A_z = 2\pi\ 103\text{x}10^6$ rad/s

I(+1) = 13.5, I(0) = 16.4, I(-1) = 3.4 (arbitrary units)

$\Delta B_o = 3.52$ Gauss $\beta = 9.274\text{x}10^{-21}$ erg/G

$\nu = 9.2449\text{x}10^9\ s^{-1}$ $h = 6.626\text{x}10^{-27}$ erg s

$\tau = 2.1\text{x}10^{-9}$ s from B or $\tau = 2.3\text{x}10^{-9}$ s from C

The disagreement is an indication of the approximate nature of this calculation. State-of-the-art calculations incorporate detailed physical models.

Slower Tumbling

When tumbling is slower than that required for motional narrowing or tumbling is anisotropic, determination of the tumbling correlation time is best done by lineshape simulation. The results are model dependent.

When a spin label is attached to a protein, rotation of the probe with respect to the protein surface may not be possible through a full 360^{o} and may be highly anisotropic. Freed and his colleagues have modeled these spectra in terms of microscopic order/macroscopic disorder (MOMD).

Extensive discussion of these cases can be found in:

J. H. Freed, Theory of Slow Tumbling ESR Spectra for Nitroxides, *Spin Labeling Theory and Applications*, Academic Press, 1976, ch. 3.
D. E. Budil, S. Lee, S. Saxena, and J. H. Freed, Nonlinear-least-squares analysis of Slow-Motion EPR Spectra in One and Two Dimensions Using a Modified Levenberg-Marquardt Algorithm, *J. Magn. Reson*. **A120**, 155-189 (1996).

Oximetry

Collisions with paramagnetic oxygen molecules decrease T_{1e} and T_{2e}. This is analogous to the use of paramagnetic metals as NMR relaxation enhancement reagents. For narrow-line EPR signals the decrease in T_{2e} causes line broadening, which can be avoided by degassing the sample.

The broadening of narrow-line EPR signals by oxygen can be used to monitor oxygen concentration, which is called oximetry, and is being developed as in *in vivo* monitoring technique.
The oxygen transport parameter, W, is defined as

$$W = T_1^{-1}(\text{air}) - T_1^{-1}(N_2)$$

and is proportional to the local diffusion coefficient of oxygen.

A. Kusumi, W. K. Subczynski and J. S. Hyde, *Proc. Natl. Acad. Sci*. 79, 1854-1858 (1982).

K. Kawasaki, J.-J. Yin, W. K. Subczynsk, J. S. Hyde, A. Kusumi, *Biophys. J.* **80**, 738-748 (2001).

Oxygen Accessibility

Accessibility of nitroxyl spin labels to collisions with oxygen can be used to distinguish between buried and surface exposed sites on a protein. Measurements could be done by time domain methods, but so far have been done by CW saturation. The accessibility parameter Π is defined as:

$$\Pi(O_2) = \frac{\Delta P_{1/2}(O_2)}{P_{1/2}(DPPH)} \frac{\Delta H_o(DPPH)}{\Delta H_o}$$

DPPH is used as a standard for calibration for the product, T_1T_2.

$P_{1/2}$ is the microwave power that causes the amplitude of an EPR signal to be half of that predicted in the absence of power saturation.

$\Delta P_{1/2}(O_2) = P_{1/2}(O_2) - P_{1/2}(N_2)$

$\Delta H_o(DPPH)$ is the peak-to-peak linewidth of crystalline DPPH (2,2-diphenyl-1-picrylhydrazyl)

ΔH_o is the peak-to-peak linewidth of the central nitroxyl line, which is a qualitative indicator of mobility. As motion slows, ΔH_o increases.

See H. S. Mchaourab and E. Perozo, *Biol. Magn. Reson*. **19**, 185-247 (2000) and references therein.

Oxygen Accessibility

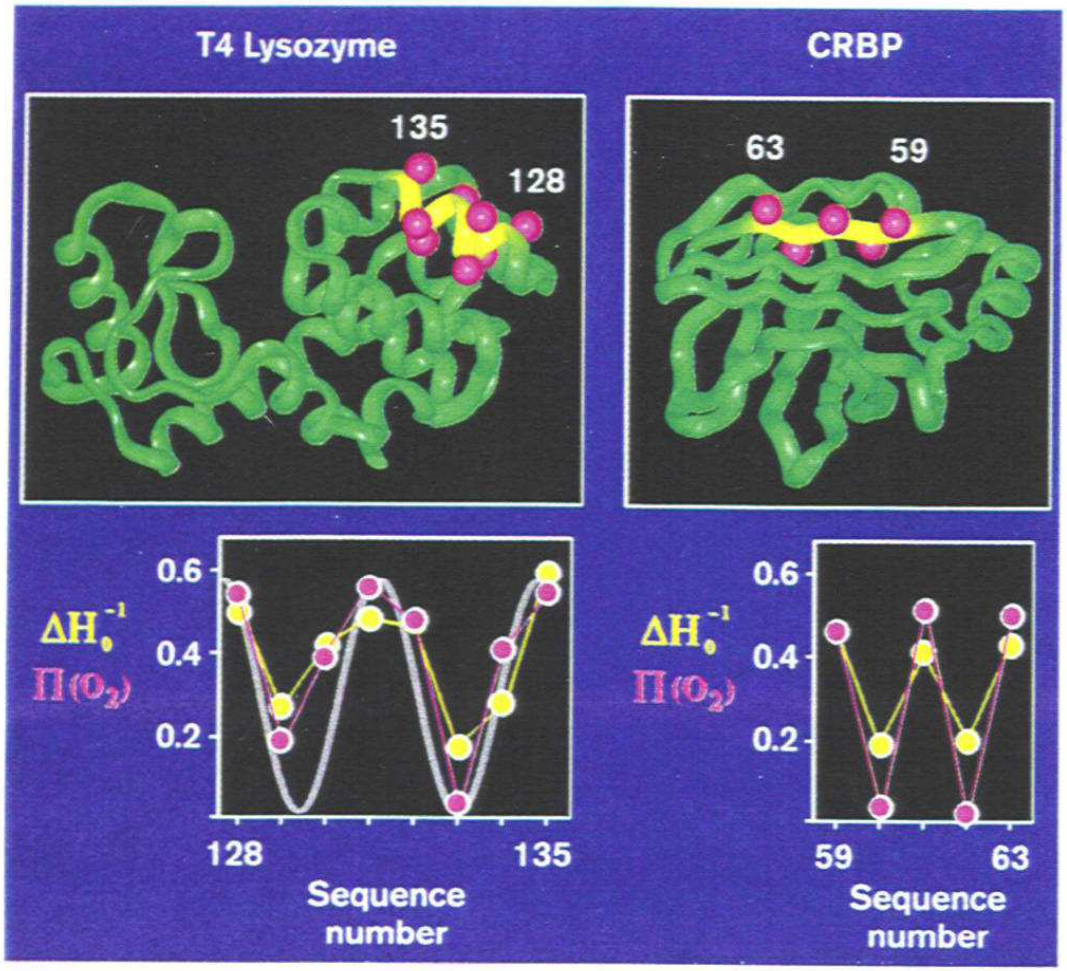

Oxygen accessibility and probe mobility were measured as a function of sequence number for spin labels attached to T4 lysozyme (T4L) and cellular retinol binding protein (CRBP).
The correlation between the two parameters indicates that the most mobile sites are also the most oxygen accessible.
The repeat period of about 3.6 for T4L is consistent with the α-helical structure of this segment of the protein.

W. L. Hubbell, H. S. Mchaourab, C. Altenbach, and M. A. Lietzow, *Structure* **4**, 779-783 (1996).

Molecular Tumbling Induces Relaxation

Molecular tumbling induces relaxation in S=1/2 systems by

- spin rotation
- modulation of g anisotropy
- modulation of hyperfine anisotropy

Each of these contributions has a characteristic dependence on tumbling correlation time and microwave frequency. Very few species have been studied as a function of temperature or tumbling correlation time, so it is not known which terms dominate for various classes of radicals.

$$\frac{1}{T_{1e}} = \frac{A_{SR}}{\tau_R} + (A_g + A_a)\frac{\tau_R}{1+\omega_e{}^2\tau_R{}^2}$$

τ_R is the tumbling correlation time
A_{SR} is the coefficient for spin rotation and is proportional to $(g-g_e)^2$
A_g is the coefficient for modulation of g anisotropy, which is proportional to g anisotropy squared, and to $\omega_e{}^2$
A_a is the coefficient for modulation of hyperfine anisotropy, which is proportional to hyperfine anisotropy squared, and is independent of ω_e

P. W. Atkins, in *Electron Spin Relaxation in Liquids*, Muus and Atkins, eds., Plenum, N. Y., 1972, p. 279.
D. Kivelson, *J. Chem. Phys*. **33**, 1094 (1960).

Semiquinones

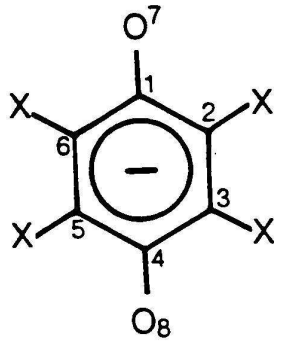

X= Cl, Br

X=Cl, g=2.0083, 2.0065, 2.0021
X=Br, g=2.0142, 2.0098, 2.0014

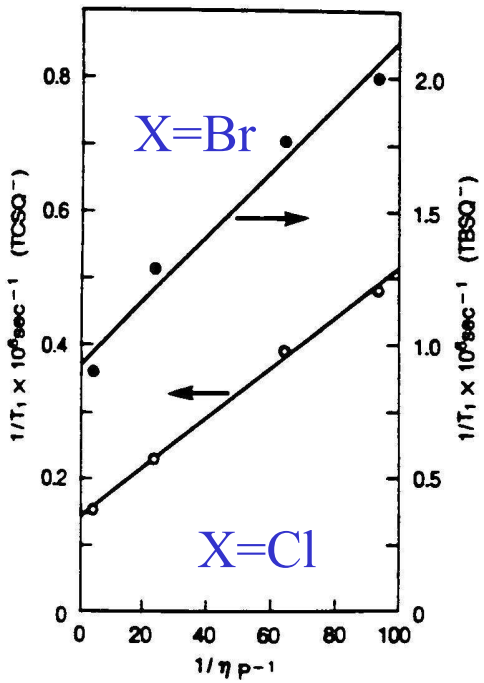

By SR

Viscosity, η, was varied by changing the composition of ethanol:glycerol mixtures at constant temperature. The tumbling correlation time, τ, is expected to be linearly related to η so the linear dependence of $1/T_{1e}$ on 1/ η is consistent with spin-rotation. g-values are further from 2.0023 for X=Br than for X = Cl, so the faster relaxation for X = Br than for X = Cl also is consistent with spin rotation.

Power saturation curves demonstrated that relaxation was independent of microwave frequency, which is not consistent with modulation of g and/or A anisotropy.

B. S. Prabhananda and J. S. Hyde, *J. Chem. Phys*. **85**, 6705 (1986).

Triarylmethyl Radicals

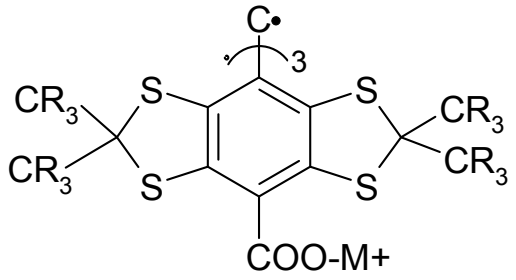

sym-trityl-CH_3 R = H, M = Na^+

sym-trityl-CD_3 R = D, M = K^+

For these radicals g-values are close to 2, and the hyperfine coupling is weak. As a result, spin rotation and modulation of g and/or A anisotropy are not expected to be effective relaxation mechanisms.

Values of T_{1e} in mixtures of water:glycerol showed little dependence on viscosity or on microwave frequency between 250 MHz and 9.5 GHz, which indicates that spin rotation and modulation of g and A anisotropy do not dominate the relaxation, consistent with expectation.

L. Yong et al., *J. Magn. Reson*. **152**, 156 (2001).

Triarylmethyl Radicals

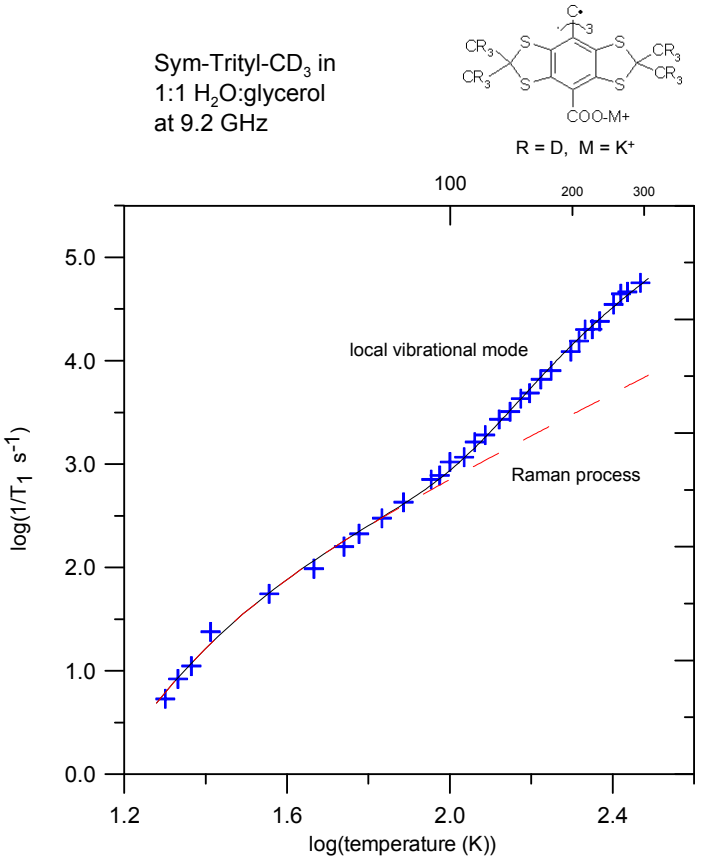

Values of T_{1e} measured by saturation recovery or inversion recovery were the same, within experimental uncertainty, which indicated the absence of spectral diffusion processes.

The 1:1 water:glycerol glass melts at 200 K, but there is no change in the slope of the plot of $1/T_{1e}$ vs. T, consistent with the room temperature measurements that indicated no dependence on tumbling correlation time.

The temperature dependence is consistent with a Raman process at low temperature plus a local vibrational mode at higher temperature. The energy for the local mode is consistent with that for the C-S stretch.

Nitroxyl Radicals – T_m

~ 330 K

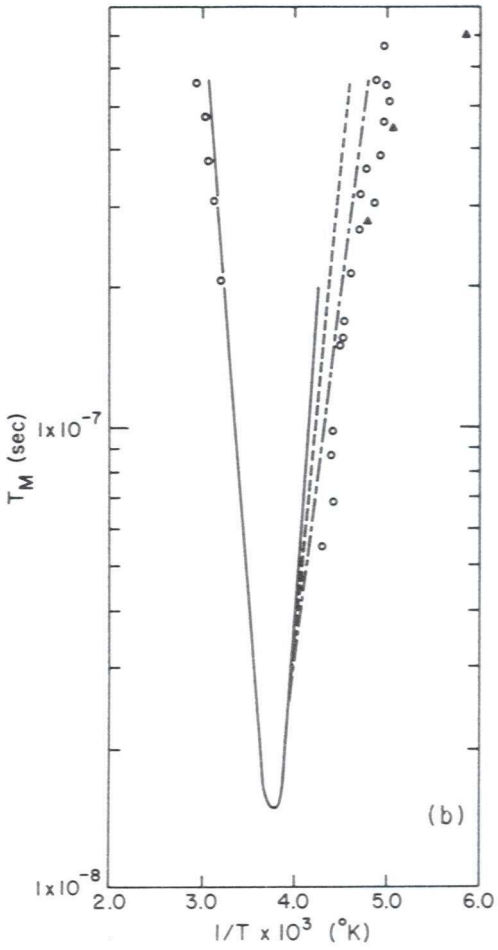

← Temperature

Values of T_m for tempone in 85% glycerol:15% water obtained by
(O) two-pulse spin echo data
(Δ) 2D- ESE contour plots
The three lines show the calculated values based on jump diffusion (__), free diffusion (_ _) and Brownian diffusion (_ . _ .).

In the intermediate tumbling regime T_m for a nitroxyl radical is too short to measure by current spin echo techniques.

G. L. Millhauser and J. H. Freed, *J. Chem. Phys*. **81**, 37 (1984).

$N@C_{60}$

This is a special case of atomic spectroscopy in condensed phase.
The EPR lines are very narrow because there are few neighboring nuclei with a spin.
The N ground state is $^4S_{3/2}$ and the hyperfine splitting is isotropic.
T_1 of $N@C_{60}$ was about 200 μs in polycrystalline C_{60} at room temperature.
In solution the central line exhibited an ESE decay constant of 120 μs, and T_1 was found to be equal to T_2.
Demonstration that the relaxation of $N@C_{60}$ in solution was a thermally-activated process, attributed to collisional modulation of ZFS for the S=3/2 center, was provided by the observation that T_{1e} at 95 GHz was four times longer than at 9.5 GHz. The data fit the following expression, which was derived for S = 3/2 (l = 1,2):

$$\frac{1}{T_1(\ell)} = \frac{12}{15} D^2 \left(1 + \frac{\eta^2}{3}\right) \frac{\tau}{1 + (\ell\omega\tau)^2}$$

where D is the ZFS parameter, η is the asymmetry parameter, and τ is the time of the fluctuating process.

C. Knapp, N. Weiden, and K.-P. Dinse *Appl. Phys. A. Mater. Sci. Process.* **66**, 249-255 (1998).
N. Weiden, H. Käss, K.-P. Dinse *J. Phys. Chem. B.* **103**, 9826-9830 (1999).

Summary of Temperature Dependence

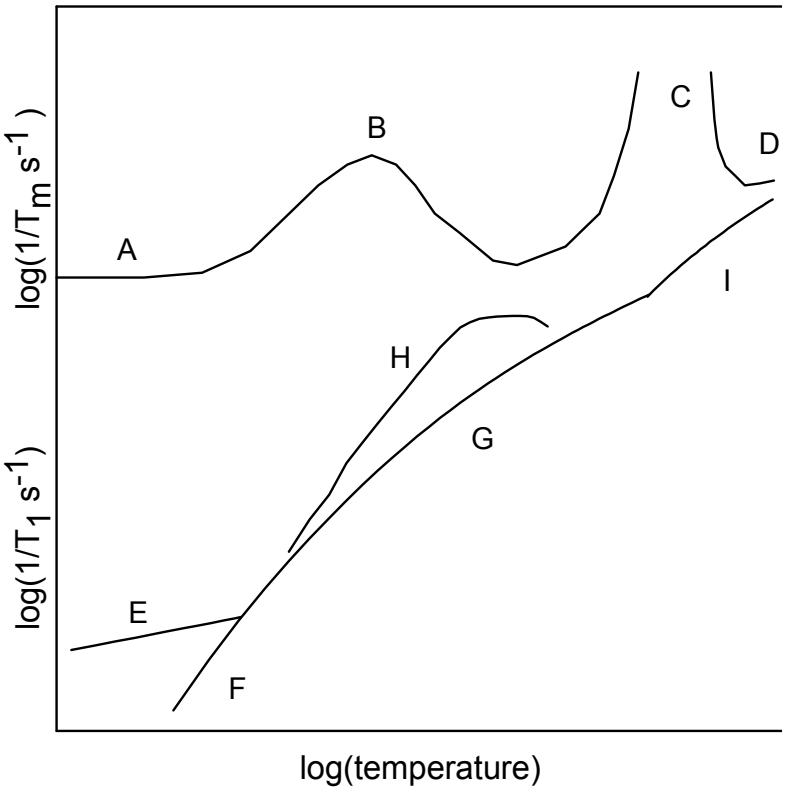

Temperature dependence of relaxation rates observed when

T_m is dominated by:

A nuclear spins in the surroundings

B collapse of couplings to methyl groups or rapidly relaxing spin

C averaging of g- or A-anisotropy

D T_1

T_1 is dominated by:

E direct process and/or high spin concentration

F, G Raman or Orbach process

H interaction with a more rapidly-relaxing electron spin

I local mode, thermally-activated process, modulating spin-orbit coupling or ZFS

Contributions to T_1

- vibrations anisotropically modulate spin-orbit coupling, and mix spin and orbital angular momentum
- hence, for axial symmetry, T_1 is shortest in the xy plane, and longest along z
- vibrations of the molecule exchange energy with the lattice
- collisions of the molecule with solvent (including in frozen solution) excite vibrations of the molecule
- at ca. 100 K in a "frozen" solution a molecule undergoes low-amplitude molecular motions many times during T_1
- in a "rigid" lattice energy can be exchanged with the lattice via
  - a single resonant phonon – direct process
  - two phonons – Raman process
  - excited state electronic energy level within the phonon bath – Orbach process
  - excited state vibrational energy level within the phonon bath – Murphy process
  - local vibrational mode
  - special vibration/phonon interactions also are possible
- temperature dependence can be complicated, and includes linear ($T_1 \alpha T^{-1}$) to $T_1 \alpha T^{-9}$, but is commonly $T_1 \alpha T^{-n}$ with n = 2 to 3 from ca. 10 K to the melting point of the solvent.
- spin-spin interaction with a faster-relaxing electron spin

Contributions to T_m

- T_2 = electron spin-spin relaxation
- Instantaneous diffusion. The second pulse flips a neighboring spin.
  - The process has larger impact for
    - higher spin concentrations,
    - narrower EPR signals, and
    - larger microwave B_1
- Intramolecular dynamic processes
  - small amplitude motion
  - rotation of methyl groups to which the unpaired electron is coupled
  - relaxation of spin-coupled systems
- Averaging of g and A anisotropy by molecular tumbling
- Nuclear spins in the surroundings

Summary of Relaxation Mechanisms

The spin angular momentum of the A spins is mixed with other angular momenta by spin-orbit coupling or spin-rotation coupling. The time-dependence of the mixing of angular momenta, occurs by

- rotational motion
- motional modulation of dipolar coupling
- mixing of excited states (e.g. by conformational changes)
- thermal motions modulating zero-field splitting

This mixing of angular momenta is thermally activated, and provides a mechanism for coupling the spin angular momenta to the thermal energy of the lattice.

Relaxation Mechanisms

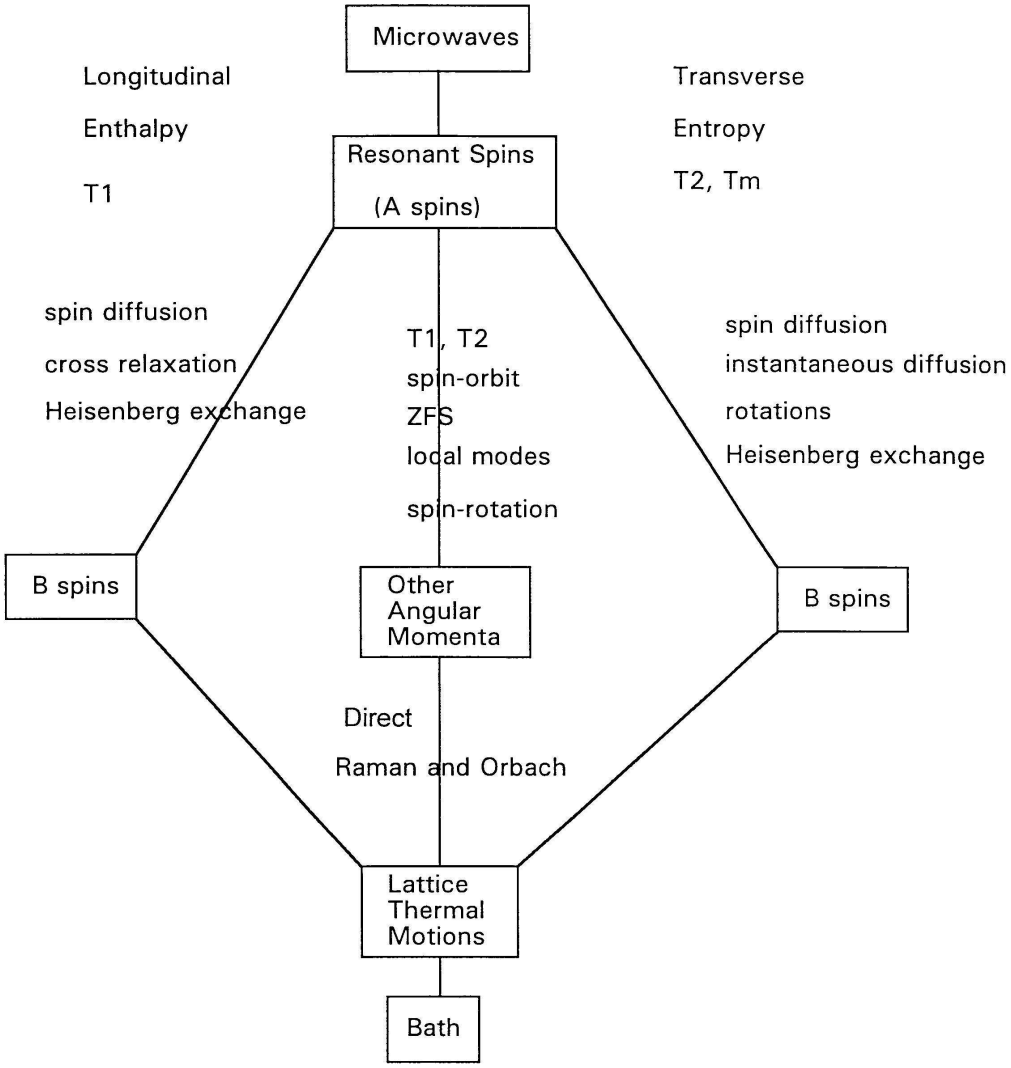

Further Reading on Electron Spin Relaxation Times

Abragam, A., and Bleaney, B. (1970) *Electron Paramagnetic Resonance of Transition Ions*. Oxford University Press, London.

Bertini, I., Martini, G., and Luchinat, C. (1994a) Relaxation, Background and Theory, in *Handbook of Electron Spin Resonance*. Poole, C. P., Jr., and Farach, H. A. eds, American Institute of Physics, New York, 51-77.

Bertini, I., Martini, G., and Luchinat, C. (1994b) Relaxation Data Tabulation, in *Handbook of Electron Spin Resonance*. Poole, C. P., Jr., and Farach, H. A. eds, American Institute of Physics, New York, 79-310.

Bowman, M. K., and Kevan, L. (1979) Electron Spin-Lattice Relaxation in Nonionic Solids, in *Time Domain Electron Spin Resonance*, L. Kevan and R. N. Schwartz, eds., Wiley, New York, pages 68-105.

Bowman, M. K. (1993) Strategies for Measurement of Electron Spin Relaxation, in *Magnetic Resonance of Carbonaceous Solids*, R. E. Botto and Y. Sanada eds., *Adv. Chem. Ser.* **229**, Chapter 5.

Eaton, S. S., and Eaton, G. R. (2000) Relaxation Times of Organic Radicals and Transition Metal Ions, in *Distance Measurements in Biological Systems by EPR*, G. R. Eaton, S. S. Eaton, and L. J. Berliner, eds., *Biol. Magn. Reson*. **19**, 29-154.

Geschwind, S., ed., (1972) Electron Paramagnetic Resonance, Plenum Press, New York.

Kevan, L., and Schwartz, R. N., eds., (1979) *Time Domain Electron Spin Resonance*, Wiley-Interscience, New York.

Standley, K. J. and Vaughan, R. A. (1969) *Electron Spin Relaxation Phenomena in Solids*. Plenum Press, New York.